Coherence between two coupled lasers from a dynamics perspective

Will Ray*

HRL Laboratories, LLC, Malibu CA 90265 and

Center for Nonlinear Science and School of Physics

Georgia Institute of Technology, Atlanta, GA 30332-0430

Jeffrey L. Rogers†

HRL Laboratories, LLC

Malibu, CA 90265

Kurt Wiesenfeld‡

Center for Nonlinear Science and School of Physics

Georgia Institute of Technology, Atlanta GA

(Dated: November 27, 2007)

Abstract

We compare a simple dynamical model of fiber laser arrays with independent experiments on two coupled lasers. The degree of agreement with experimental observations is excellent. Collectively the evidence presented supports this dynamical approach as an alternative to the traditional static eigenmode analysis of the coupled laser cavities.

*wray3@mail.gatech.edu

†jeff@hrl.com

‡kurt.wiesenfeld@physics.gatech.edu

I. INTRODUCTION

Recognizing the power limitations of individual lasers, researchers have tried to develop methods of combining light from an array of semiconductor or fiber lasers to obtain an efficient high-power source. Extensive investigations have evaluated various coupling architectures with the goal of promoting coherent addition in the far-field of the light emitted from the output reflectors of individual lasers. Inphase array emission, where all constituent lasers operate at a common frequency and with zero relative phase difference, has been demonstrated using active control of the phases [1] and with passive coupling schemes including multicore fibers [2, 3], self-Fourier cavities [4], and Talbot resonators [5, 6]. These coupling devices often suffer from alignment issues, stability problems due to low threshold differences between array solutions, or increased cavity losses in their implementation.

An alternative approach has recently been developed to enforce coherent beam combination in arrays [7–14]. In addition to a passive coupling arrangement among the elemental lasers, losses incurred at the individual output facets are purposely imbalanced. Experimental investigations have reported emission of inphase coherent light solely from the output reflector having the lowest losses. This form of single-facet emission has been studied primarily in arrays of solid-state and fiber lasers using interferometric coupling devices such as beam splitters [15, 16], fold mirrors [14], or directional couplers [8–11, 13]. In most realizations only one coupler output is fitted with a reflector to provide a global feedback for the entire array.

Although well-documented experimentally, few model descriptions have studied this configuration of coherent beam combining. In one depiction [9], the array of coupled lasers is treated as a single compound-cavity laser. The intrinsic laser dynamics are ignored and coherent beam combination is discussed in terms of the static eigenmodes, often referred to as supermodes, of the compound-cavity setup [17]. Although an analysis of these solutions provides important considerations necessary for inphase emission from a single output facet, the validity of this description is limited to continuous-wave (cw) emission for pump strengths very close to threshold. In contrast, experiments have shown high addition efficiency in pulsing Q-switched fiber lasers [18] and at pump strengths extending far above threshold where the output light often exhibits more complicated dynamics such as self-pulsing.

In this paper we investigate the phenomenon of coherent emission from a single output

facet using an iterative map model recently introduced to describe the dynamics of fiber laser arrays [19]. Simulations of two coupled lasers with experimentally derived parameters robustly produce coherent inphase emission of light entirely from the output facet with lowest losses, even when there is only a small mismatch in output losses [10]. Furthermore, the model shows excellent quantitative agreement with experimental results in the presence of an additional detuning of the individual pump currents from optimal operating conditions [7, 9].

A significant feature of the iterative map model is the treatment of each individual laser as a separate dynamical oscillator influenced by the other laser via a passive, lossless coupler. Our numerical computations are consistent with a static description of the system provided by supermode theory within the latter's range of validity. In addition, the dynamical model robustly reproduces the experimental observations over a large range of pumping values spanning both cw and pulsing dynamical regimes.

II. MODEL DESCRIPTION

The experiments we consider use the setup schematically illustrated in Fig. 1. Each laser cavity is formed by a fiber Bragg grating (FBG) providing nearly 100% reflection on one end and a high-loss output facet at the other end typically reflecting only about 4% of the incident intensity. A joint coupling region, most often manifested as a 50/50 fused fiber coupler, lies between the individual gain blocks and the output facets.

A. Iterative Maps

We recently introduced a dynamical model for a general class of fiber laser arrays which includes the setup of Fig. 1 as a special case. A set of nonlinear coupled iterative maps traces the evolution of the electric field and gain of each laser over one round trip. In a three-level lasing scheme, the forward-travelling electric fields $E_{1,2}$ and gains $G_{1,2}$ of the individual fibers, starting in Fig. 1 immediately before the output coupler, are explicitly transformed in one pass through their respective cavities according to [19, 20]

$$E_n(t+T) = e^{G_n(t)+j\phi_n^L} \sum_{\ell=1}^{2} S_{n\ell} e^{j\phi_\ell^R} r_\ell \sum_{m=1}^{2} S_{\ell m} E_m(t). \tag{1}$$

$$G_n(t+T) = G_n(t) + \epsilon \left[W_n^p \tau \left(G_{tot} - G_n(t) \right) - \left(G_{tot} + G_n(t) \right) \right] - \frac{2\epsilon}{I_{sat}} \left(1 - e^{-2G_n(t)} \right) |E_n(t)|^2 , \quad (2)$$

After an initial pass through the coupler, denoted by the matrix S in Eq. (1), the emerging electric fields propagate towards the output facets with respective reflection coefficients $r_{1,2}$. The light reflected from each output face then reenters the coupler and passes through the individual gain arms before finally arriving at the starting point. The amplification of the fields due to the back-and-forth propagation through the gain sections is characterized by exponential gains $e^{G_{1,2}}$.

In writing these equations, we have explicitly separated the total phase shift into three parts: $\phi_{1,2}^L$ is the phase shift acquired during transit through the individual gain arms on the left-hand side of the coupler; $\phi_{1,2}^R$ denotes the phase shift picked up from propagation through the region on the right-hand side of the coupler; and the phase shift gained in the coupling region is contained in the coupling matrix S. This separation of the acquired phase shifts is important when we consider the conditions for emission from a single facet when an imbalance exists in the losses from the individual output facets.

The evolution equation for the gain, Eq.(2), details operation of a fiber laser in a three-level scheme [20]. We adopt this form since the experiments we consider used erbium-doped fiber lasers. The pumping rate $W_{1,2}^p = C^p P_{1,2}$ is linearly proportional to each laser diode pump current $P_{1,2}$ for a pumping efficiency C^p. The total available gain in each laser G_{tot} is proportional to the stimulated emission cross section and obtainable population inversion. The parameter ϵ sets the time scale for the gain dynamics and is the ratio of the round trip time in the cavity to the fluorescence time of the inversion. The saturation intensity I_{sat} dictates the average power emitting from each fiber laser.

B. Coupling

Although many optical devices have been developed to couple light between individual lasers, directional couplers are often used since it is not necessary for light to enter or exit the optical waveguides in any part of the array. These evanescent couplers are typically formed by placing the cores of two fibers close enough together over an interaction region d so that light is able to leak from one into the other.

We have previously derived a general formulation to describe passive linear coupling for an arbitrary number of interacting fibers [19]. A directional coupler between two waveguides may be succinctly characterized by the propagation constants $\beta_{1,2}$ for light remaining within a given fiber through the coupling region and the propagation constants κ_{12} and κ_{21} describing the perturbation of light entering from the other fiber. For a symmetric coupler with $\beta_1 = \beta_2 = \beta$ and $\kappa_{12} = \kappa_{21}^* = \kappa$ (a real constant in a loss-less coupler), the coupling matrix S may be written as

$$S = e^{j\beta d} \begin{pmatrix} \cos(\kappa d) & j\sin(\kappa d) \\ j\sin(\kappa d) & \cos(\kappa d) \end{pmatrix}. \tag{3}$$

In this form it is clear that the light sloshes back-and-forth through the coupling region as a function of the interaction length. While it is difficult to experimentally determine the overall phase βd acquired in the coupler, one may easily characterize κd by measuring how power entering from one fiber distributes to the two output fibers. We consider 50/50 power splitters in this study, which requires κd to be an odd multiple of $\frac{\pi}{4}$. Any odd multiple may be used in the simulations, as other choices only differ by an overall phase shift that may be absorbed into βd.

III. COHERENT BEAM COMBINATION

Inphase combination of light from two coupled fiber laser elements out of a single output facet was first reported by Lyndin *et al.* in 1994 [7]. Since then a number of research groups have observed this phenomenon using a variety of coupling configurations. Kozlov *et al.* enforced coherent addition between two lasers by forming a common output facet from one half of a directional coupler [8]. A majority of investigations have been performed, however, using a setup similar to the one in Fig. 1. A common output facet is selected by detuning the amount of loss incurred at the two output facets. More recent studies have shown high addition efficiencies of four, five, and even eight lasers using a hierarchical nesting of 2x2 couplers [10, 13].

In this section we compare predictions of the iterative map model, Eqs. (1,2), with experimental realizations of this system. The first step is to set the model parameters (see Table I).

TABLE I: Parameter values used for simulations of two coupled lasers. The operating conditions are estimated from an empirical characterization of this system found in Ref. [9].

Parameter	Description	Value	Units
ϵ	ratio of round-trip to fluorescence time	1.632×10^{-5}	dimensionless
G_{tot}	total linear gain	8	dimensionless
C^p	pumping efficiency	603	$A^{-1}s^{-1}$
$W^p_{1,2}$	pumping rate	varies	s^{-1}
$r_{1,2}$	output facet reflectivity	varies	dimensionless

A. Model Parameters

We use the information supplied by Simpson *et al.* for their system of two lasers linked by a single directional coupler [9]. Two high-gain erbium-doped fibers were joined with a 50/50 coupler and capped on the one end with high-reflecting fiber Bragg gratings. The lengths of the two fiber arms containing the gain elements were approximately 14 m but were not identical. One of the two coupler outputs was flat-cleaved providing a reflection of 4% of the intensity back into the cavity while the other was angle-cleaved to minimize any back reflection. Each output fiber had a length of roughly 2 m.

With a reported single pass gain of 40 dB in each active gain medium, the total linear gain parameter may be estimated as $G_{tot} = 8$ [9]. Since the vast majority of the losses occur from the output facets, we set the field reflection coefficients to be $r_1 = 0.20$ for the flat-cleaved output facet and $r_2 = 0$ for the laser with the angle-cleave. The round-trip time of the each cavity $T = 163.2$ ns is computed using an index of refraction of 1.53 and total length of 16 m. Taking a fluorescence time of 10 ms for each erbium-doped fiber yields an estimate of $\epsilon = 1.632 \times 10^{-5}$. A pumping efficiency $C^p = 603$ is chosen to match the lasing threshold of the model with the experimentally determined threshold laser diode pump current. We set $I_{sat} = 1$ since measurements of the output intensity in this experiment are reported in terms of voltages recorded by the detection equipment and we do not have direct knowledge of the output powers.

As discussed in the previous section the coupling parameters must be selected to produce the power splitting effects of a 50/50 directional coupler. Consequently we choose $\kappa =$

0.001 μm^{-1} and $d = 13351.7646\ \mu m$. Additionally, we set $\beta = 8\ \mu m^{-1}$ although this propagation constant is arbitrary and its value does not affect the output of the system. Likewise, the phase shifts incurred during back-and-forth propagation through the arms with the output facets do not alter the dynamics and we set $\phi_1^R = \phi_2^R = 0$. However, the choice of the phase shifts obtained during transit through the two gain arms are important. In particular, the *relative phase shift* $\Delta\phi^L = \phi_2^L - \phi_1^L$ must be equal to an odd multiple of π in order for the light to be effectively funnelled into only the output facet with the lower losses. The absolute phase shift of either arm is arbitrary and so we set $\phi_1^L = \pi$ and $\phi_2^L = 0$.

B. Power Extraction

With the model parameters determined, we are now ready to investigate numerically the phenomenon of coherent beam combining. For reference we first consider the dynamics and power output characteristics of a single fiber laser detached from the coupler with a back reflection of 4% of the incident intensity at the output facet. The average intensity output for this individual laser as a function of laser diode pump current is shown by the solid line in Fig. 2(a). Emission in the cw state is observed after the diode pump is tuned past 0.25 A. This diode pump strength corresponds to a pumping rate $W^p = 150.8$. The cw state persists only near threshold and the intensity and gain dynamics exhibit self-pulsing once the diode pump current is tuned past 0.28 A. As pump current is further increased the height and frequency of the pulses rise linearly while the width of an individual pulse decreases.

We next consider two coupled lasers symmetrically pumped for increasing levels of diode pump current. The power extracted from the two output ports is displayed by the circles in Fig. 2(a). The filled circles represent the average intensity emanating from the flat-cleaved output facet associated with the first laser, while the open circles depict the average intensity from the very high-loss angle-cleaved output facet of the second laser. We see that all light emits from the flat-cleaved output facet with the lowest losses, and no light is observed from the angle-cleaved output facet. Comparison with the individual laser extraction shows that, although both have the same lasing threshold, the slope efficiency of the symmetrically pumped lasers is twice that of the single laser demonstrating a 100% combining efficiency. The onset of pulsing in the intensity dynamics occurs at the same diode pump current as the individual laser, a result found in previous simulations of the iterative map model with

identical output facet reflection coefficients [19].

The results of Fig. 2(a) are in agreement with experimental power extraction curves showing combining efficiencies up to 99% [11]. Figure 2(b) plots an extraction curve obtained from experiments on a pair of coupled high-power erbium-doped fiber lasers with imbalanced losses at the output ports [21]. The filled (open) circles represent the average power emitting from the output port with lower (higher) losses, while the solid line depicts the emission from an individual laser. The lasers are symmetrically pumped far above threshold level, yet coherent beam combination of the light from the lower-loss output facet persists over all considered input pump powers with a combining efficiency of 93%.

In experimental studies of coherent beam combining the power output of symmetrically pumped lasers is typically compared to the power extraction when only one component laser of the array is pumped. This scheme is distinct from the individual laser as light coupled into the unpumped laser results in additional losses. The power extraction of each output port in this case is shown by the dashed line in Fig. 2(a). The flat- and angle-cleaved facets each emit roughly a quarter of the average intensity obtained from the flat-cleaved output in the case of symmetrically pumped lasers in agreement with experimental observations [9]. For the iterative map model this fraction is less than four over the range of pump currents investigated due to two effects related to the additional loss into the non-pumped component laser cavity. First, the threshold gain is increased by a factor of ln(0.5) and consequently emission does not begin until the pump is raised 20% beyond the individual laser threshold. In addition, the losses from the coupler lower the slope efficiency of the component laser. As a result, pulsing is not observed to occur until the diode pump current is raised above 0.36 A.

C. Detuning of the Pump Sources

In the previous section the lasers were operated in a symmetrical fashion, including equal levels of pumping applied to each fiber arm. We now examine what happens when there is a mismatch in the individual diode pump currents. For comparison in Fig. 3(a) we reproduce the data shown in Fig. 4(b) of Ref. [9], an experimental realization of pump mismatch obtained using two coupled erbium-doped fiber lasers. In the experimental extraction curve, the first erbium-doped fiber laser is pumped at a fixed level of 0.46 A while the second pump

is tuned from 0 A to a maximum value of 0.70 A. In this plot the filled circles represent emission from the flat-cleaved output facet while the open circles depict the intensity from the angle-cleave of the second laser. When the second laser diode pump current is less than 0.30 A, the lasing threshold of a component laser, the two output facets emit with equal intensity levels. At higher pumping rates the flat-cleaved light output is seen to increase linearly while the angle-cleaved output tends toward zero. After the second diode pump current is raised above the fixed pump level of the first laser, the intensity emerging from the angle-cleaved output is observed to increase.

Figure 3(b) shows the extraction curve we find from simulations of Eqs. (1,2). As in the experiment, the pump current of the first laser is set to a fixed value of 0.46 A; high enough that the intensity dynamics are in the pulsing regime for all pump levels investigated. All other model parameters remain as before. The filled circles represent emission from the output port terminated by a flat-cleave and the open circles show the intensity from the angle-cleave. It is immediately clear that the intensity from the angle-cleaved port follows a trend similar to the experimental measurement. A minimum in this output is realized when the two laser diode pump currents are identical. When the second diode laser is pumped at the maximum current of 0.70 A, we find that the ratio of the average intensity from the angle-cleaved output to the flat-cleaved port is a factor of two smaller than the experimental result, producing reasonable quantitative agreement between the model and experiment.

The emergence of light from the angle-cleaved output port for detuned diode pump currents can be explained by a linear analysis of interference in the 50/50 coupler [12]. When light from back-reflection off the output port splits equally into the two gain sections, the intensities are magnified by different amounts. Following amplification, the contrast of the imbalanced intensities reentering the coupler towards the output reflector results in incomplete destructive interference into the angle-cleaved output port.

The main difference between the experimental and computed extraction due to pump detuning is the pump current strength where the average intensity emitting from the two output ports begins to split. In the simulation this occurs at 0.10 A, a much lower value than the experimentally observed level of 0.30 A at the component laser threshold. The split in the output power from each facet results from interference in the coupling region of light entering in from the two laser arms. For experimental realizations of fiber lasers operating in a three-level scheme, heavy losses of the propagating electric field occur in regions of the gain

element driven below lasing threshold. Even a small net amplification of light is not present in the under-pumped laser arm until lasing threshold is reached. The model equations do not account for loss mechanisms in under-pumped three-level lasers. The split in the average simulated intensity emitting from the output ports therefore starts at sub-threshold levels due to a net amplification of the light in the under-pumped laser arm.

D. Detuning of the Output Facet Losses

So far we have investigated a special case of imbalanced losses at the two output facets. Namely, there is only a single output facet providing feedback of light to the two cavities; the other port is angle-cleaved so that effectively all approaching light is transmitted out of the system. In essence this is a single compound-cavity laser with a shared output facet and it is unclear that the two lasers in the model need be viewed as two separate but coupled oscillators.

On the other hand, a recent experimental investigation of two coupled erbium-doped fiber lasers demonstrated that coherent addition of light from a single output port is a general phenomenon which emerges even when the field reflection coefficients of the two output ports are only slightly different [10]. Using an experimental setup similar to Fig. 1 with two output facets exhibiting similar losses at a fixed level of identical pumping in each constituent laser, the losses in the lower-loss output arm were gradually increased until the total loss in this fiber port exceeded those of the other output facet. The observed average intensity from each output facet is displayed in Fig. 4(a) as the applied loss in the lower-loss arm (filled circles) is increased from 0% to 20%. The losses in the second fiber port (open circles) are fixed at a level of 9% higher than the lower-loss fiber port without applied loss. For a large detuning between the losses in output arms, the entirety of the emitted light was seen to reside in the output port with the lowest level of loss. Close to the transition point at 9% applied loss, the power measurements were unstable and light emerged from both output facets.

To replicate this experiment, we use the same model parameters as in Table I except that we now use one of the reflection coefficients as a control parameter. In particular, we leave $r_1 = 0.2$ for the flat-cleaved output face and now set $r_2 = 0.1908$ to produce a 9% greater loss of intensity at the output face. The simulated diode pump level is set to 0.46 A for each

laser where the intensity dynamics show self-pulsing.

In Fig. 4(b) we plot the simulation results as r_1 is decreased from 0.2 to 0.179, representing a 20% increase in the losses from this output port. The filled (open) circles represent the intensity emitted from the output facet of the first (second) laser. There is excellent agreement with Fig. 4(a), and a sharp transition in the emission characteristics occurs once the losses in the first laser are greater than 9%. When the losses between the two lasers differ by less than 1%, the transients of the intensity in the simulations are very long but eventually the system settles down to emission from just one output port.

The unstable emission characteristics experimentally observed in the transition region may be captured by the addition of a small amount of Langevin noise to the electric field map Eq. (2). Figure 4(c) plots the average intensity measured from each output facet for a noise amplitude of 0.02. The addition of noise provides a smoothing effect in the transition region and one output facet is no longer completely dominant. In Fig. 4(d) we show a simulated intensity time series for an applied loss of 8%. The thin (thick) line denotes the intensity from the first (second) laser. The first laser emits a majority of the system output. The light from the second laser behaves more erratically and the pulses occasionally reach higher intensities than those emitting from the first laser.

IV. DISCUSSION: STATIC VS. DYNAMIC PERSPECTIVES

The coherent addition of lasers observed in these kinds of experiments is traditionally interpreted within a static framework of coupled optical waveguides without any regard to the amplification of the light in the gain medium. The stripped-down coupled cavity is then treated as a single entity, and the resulting eigenmodes of the system, sometimes called supermodes, are then analyzed as the basis to describe the observed dynamics in the laser. It is typically postulated that the lowest loss supermode will "win" by emerging as the stable state, although growth or decay of individual eigenmodes are rarely quantified.

For example, when two coupled lasers are identical except for an imbalance in the output facet reflection coefficients, it is intuitive that losses can be minimized if all of the light is funneled to the output port with the higher reflectivity. When the cavity conditions are specified such that the light propagating back-and-forth through the two (now passive) gain arms capped with 100% reflectors pick up a relative phase shift of π, then two constructive

supermodes result which funnel light to either one or the other output port [10]. The supermode associated with the lower-loss output port retains more light each round-trip and consequently will be selected by the laser system. In fact, this supermode will be globally selected over other supermodes formed from other cavity configurations where the relative phase shift in the gain arms is not equal to π, since for these non-optimal relative phase shifts light will invariably be funneled to the higher-loss port.

The current description offers an alternative to this static perspective. We have shown that including gain as a dynamical variable and treating each laser as a separate oscillator does equally well at predicting the experimentally observed behavior in the linear (cw) regime. In addition the dynamical model also extends correct predictions far beyond threshold and even into the pulsing regime. Indeed, the coupling between the two lasers tends to align the pulse bursts of the individual lasers so that constructive interference is achieved in the coupler at all times. These observations demonstrate the importance of a dynamical model in developing an understanding of organized behavior in coupled laser systems.

We thank Akira Shirakawa for valuable discussions and providing his original data for our use. This work was supported by the High Energy Laser Joint Technology Office and the US Army Research Office under Award No. W911NF-05-1-0506. Any opinions, findings, and conclusions or recommendations expressed in this publication are those of the authors and do not necessarily reflect the views of the High Energy Laser Joint Technology Office or the Army Research Office.

---

[1] A. Liem, H. Limpert, and A. Tünnermann, "100W single-frequency master-oscillator fiber power amplifier," *Opt. Lett.*, vol. 28, no. 17, p. 1539, 2003.

[2] P. Cheo, A. Liu, and G. King, "A high-brightness laser beam from a phase-locked multicore Yb-doped fiber laser array," *IEEE Photonics Technol. Lett.*, vol. 13, no. 5, pp. 439–441, May 2001.

[3] E. Bochove, P. Cheo, and G. King, "Self-organization in a multicore fiber laser array," *Opt. Lett.*, vol. 28, pp. 1200–1202, 2003.

[4] C. Corcoran and F. Durville, "Experimental demonstration of a phase-locked laser array using a self-Fourier cavity," *Appl. Phys. Letters*, vol. 86, no. 20, p. 201118, 2005.

[5] V. Apollonov, S. Derzhavin, V. Kislov, V. Kuzminov, D. Mashkovsky, and A. Prokhorov, "Phase-locking of the 2D structures," *Opt. Exp.*, vol. 4, no. 1, pp. 19–26, Jan 1999.

[6] M. Wrage, P. Glas, and M. Leitner, "Combined phase locking and beam shaping of a multicore fiber laser by structured mirrors," *Opt. Lett.*, vol. 26, no. 13, pp. 980–982, July 2001.

[7] N. Lyndin, V. Sychugov, A. Tikhomirov, and A. Abramov, "Laser system composed of several active elements connected by single-mode couplers," *Quantum Electron.*, vol. 24, no. 12, pp. 1058–1061, 1994.

[8] V. Kozlov, J. Hernàndez-Cordero, and T. Morse, "All-fiber coherent beam combining of fiber lasers," *Opt. Lett.*, vol. 24, no. 24, pp. 1814–1816, Dec 1999.

[9] T. Simpson, A. Gavrielides, and P. Peterson, "Extraction characteristics of a dual fiber compound cavity," *Opt. Exp.*, vol. 10, pp. 1060–1073, 2002.

[10] A. Shirakawa, T. Saitou, T. Sekiguchi, and K. Ueda, "Coherent addition of fiber lasers by use of a fiber coupler," *Opt. Exp.*, vol. 10, no. 21, pp. 1167–1172, 2002.

[11] D. Sabourdy, V. Kermène, A. Desfarges-Berthelemot, L. Lefort, A. Barthélémy, C. Mahodaux, and D. Pureur, "Power scaling of fibre lasers with all-fibre interferometric cavity," *Elec. Lett.*, vol. 38, no. 14, pp. 692–693, Jul 2002.

[12] D. Sabourdy, V. Kermène, A. Desfarges-Berthelemot, L. Lefort, A. Barthélémy, P. Even, and D. Pureur, "Efficient coherent combining of widely tunable fiber lasers," *Opt. Exp.*, vol. 11, no. 2, pp. 87–97, 2003.

[13] H. Bruesselbach, D. Jones, M. Mangir, M. Minden, and J. Rogers, "Self-organized coherence in fiber laser arrays," *Opt. Lett.*, vol. 30, no. 11, pp. 1339–1341, 2005.

[14] H. Bruesselbach, M. Minden, J. Rogers, D. Jones, and M. Mangir, "200W self-organized coherent fiber arrays," in *2005 Conference on Lasers and Electro-Optics (CLEO)*, vol. 1, May 2005, paper CMDD4, p. 532.

[15] A. Ishaaya, N. Davidson, L. Shimshi, and A. Friesem, "Intracavity coherent addition of gaussian beam distributions using a planar interferometric coupler," *Appl. Phys. Lett.*, vol. 85, no. 12, pp. 2187–2189, 2004.

[16] Q. Peng, Z. Sun, Y. Chen, L. Guo, Y. Bo, X. Yang, and Z. Xu, "Efficient improvement of laser beam quality by coherent combining in an improved Michelson cavity," *Opt. Lett.*, vol. 30, no. 12, pp. 1485–1487, 2005.

[17] D. Mehuys, K. Mitsunaga, L. Eng, W. Marshall, and A. Yariv, "Supermode control in

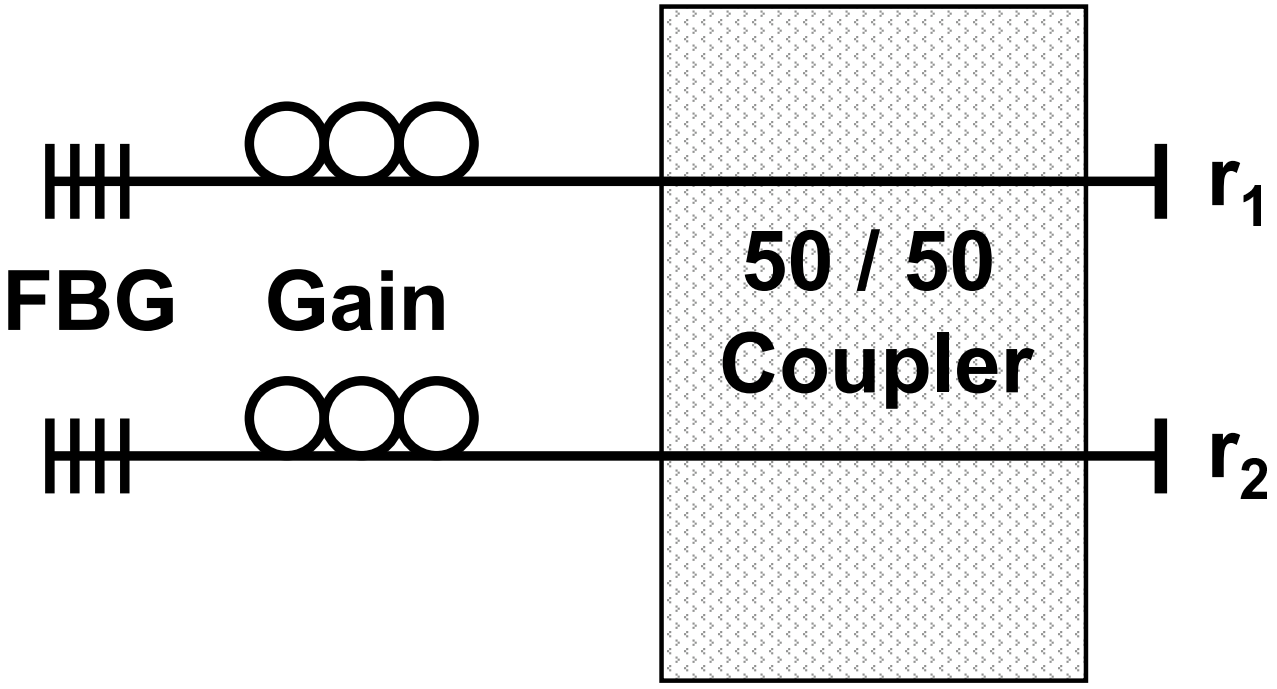

FIG. 1: Experimental schematic of two coupled lasers. Each laser gain block is terminated by a fiber Bragg grating (FBG) at one end and a high-loss output facet at the other with field reflection coefficients r_1 and r_2. A 50/50 directional coupler allows light to interact over a small distance of the fiber lengths.

diffraction-coupled semiconductor laser arrays," *Appl. Phys. Letters*, vol. 53, no. 13, pp. 1165–1167, 1988.

[18] D. Sabourdy, A. Desfarges-Berthelemot, V. Kermène, and A. Barthélémy, "Coherent combining of Q-switched fibre lasers," *Electron. Lett.*, vol. 40, no. 20, pp. 1254–1255, 2004.

[19] J. Rogers, S. Peleš, and K. Wiesenfeld, "Model for high-gain fiber laser arrays," *IEEE J. Quantum Electron.*, vol. 41, no. 6, pp. 767–773, Jun 2005.

[20] W. Ray and K. Wiesenfeld and J.L. Rogers have submitted a manuscript to be called "Refined fiber laser model".

[21] A. Shirakawa (personal communication, 2007).

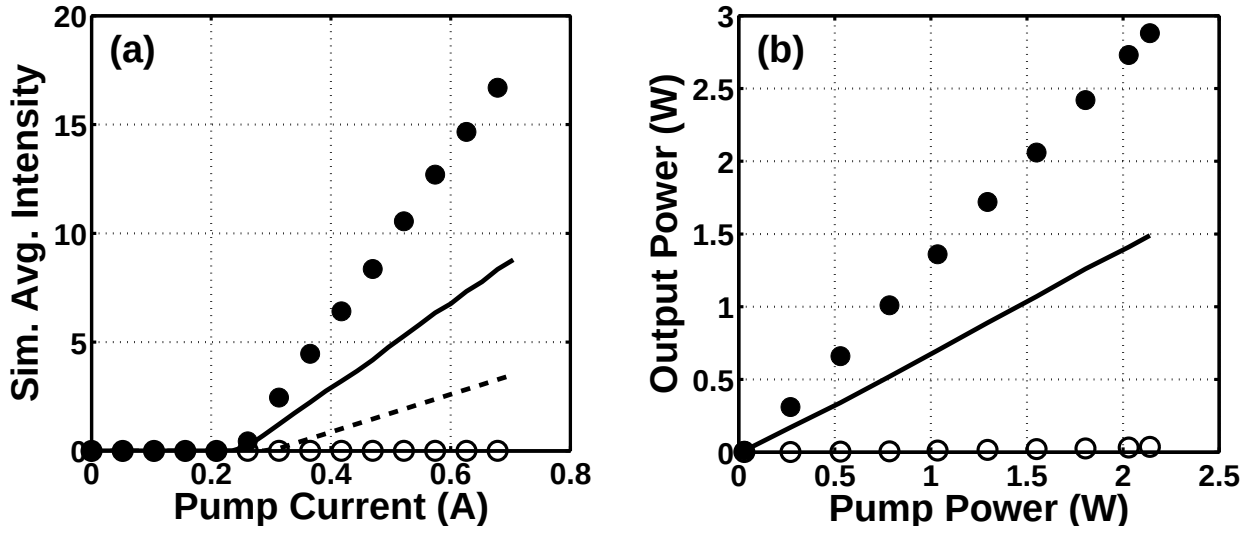

FIG. 2: Power output characteristics for individual and two coupled lasers with imbalanced losses at the output facets. The solid line represents the average intensity produced by a single laser removed from the array. The filled (open) circles represent the average intensity output from the low (high) loss output facet for two coupled and symmetrically pumped lasers. (a) Simulation using iterative map model. (b) Experiment using two coupled erbium-doped fiber lasers [21]. The dashed line in (a) shows the average intensity output from each output facet for two coupled lasers with only one component laser receiving pumping.

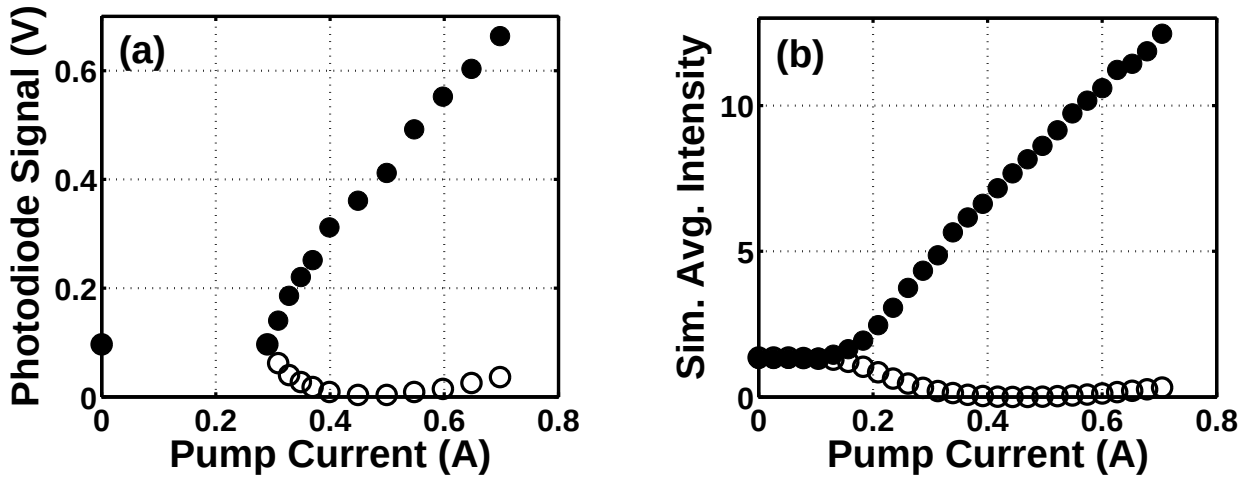

FIG. 3: Average intensity output for two coupled lasers with imbalanced losses at the output facets and asymmetrical diode pumping levels. Here the diode pump current for the first laser is fixed at 0.45 A while the second is swept from 0 A to 0.70 A. In each plot the filled (open) circles represent the average intensity emission from the lower (higher) loss output facet of the two lasers. (a) Reproduction of experimental data from Fig. 4(b) of Ref. [9]. (b) Simulation using our iterative map model.

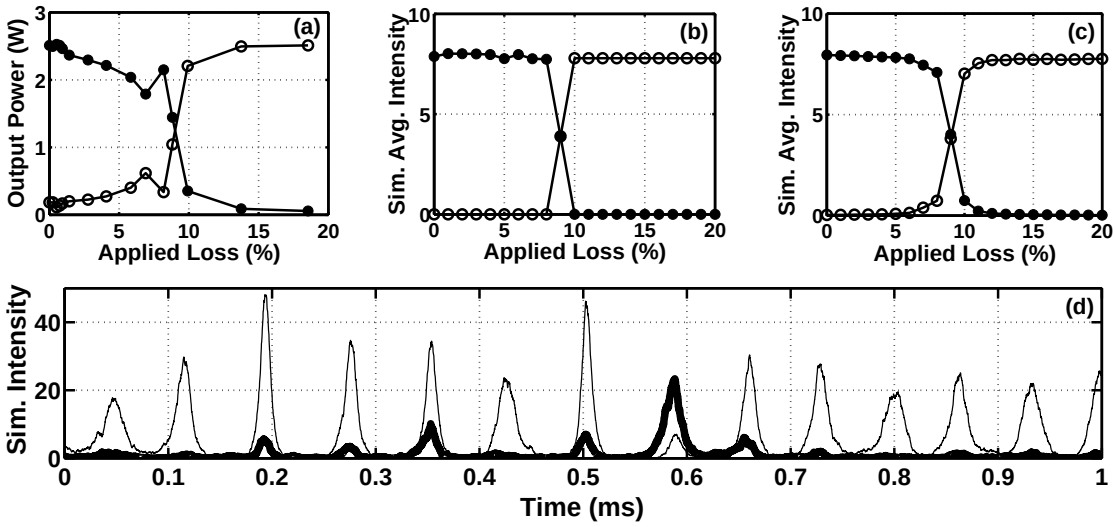

FIG. 4: (a)-(c) Plot of average intensity output as a function of the applied losses at the output facet of the first laser. The losses of the second laser are 9% higher than the losses of the first laser without applied losses. The filled (open) circles show the average intensity measured from the first (second) laser. Data shown for (a) experiment [reproduction of Fig. 4 from Ref. [10]] (b) simulation without noise (c) simulation with noise. (d) Intensity time trace from simulation with noise for applied loss level of 8%. The thin (thick) line plots pulses from first (second) laser.